JACS
JOURNAL OF THE AMERICAN CHEMICAL SOCIETY
Communication
pubs.acs.org/JACS

Termini of Bottom-Up Fabricated Graphene Nanoribbons

Leopold Talirz,*[,†] Hajo Söde,[†] Jinming Cai,[†] Pascal Ruffieux,[†] Stephan Blankenburg,[†] Rached Jafaar,[†] Reinhard Berger,[‡] Xinliang Feng,[‡] Klaus Müllen,[‡] Daniele Passerone,[†] Roman Fasel,[†,§] and Carlo A. Pignedoli*[,†]

[†]Empa, Swiss Federal Laboratories for Materials Science and Technology, 8600 Dübendorf, Switzerland
[‡]Max Planck Institute for Polymer Research, 55124 Mainz, Germany
[§]Department of Chemistry and Biochemistry, University of Bern, 3012 Bern, Switzerland

Supporting Information

ABSTRACT: Atomically precise graphene nanoribbons (GNRs) can be obtained via thermally induced polymerization of suitable precursor molecules on a metal surface. This communication discusses the atomic structure found at the termini of armchair GNRs obtained via this bottom-up approach. The short zigzag edge at the termini of the GNRs under study gives rise to a localized midgap state with a characteristic signature in scanning tunneling microscopy (STM). By combining STM experiments with large-scale density functional theory calculations, we demonstrate that the termini are passivated by hydrogen. Our results suggest that the length of nanoribbons grown by this protocol may be limited by hydrogen passivation during the polymerization step.

The lack of a band gap in the electronic structure of graphene is a major obstacle to the realization of efficient graphene-based electronic switching devices.[1] One way to open a band gap is to cut graphene into narrow ribbons. The resulting gap is approximately inversely proportional to the ribbons' width,[2] and for room temperature applications widths below 2 nm are required.[3] At this scale, the width and edge structure of the graphene nanoribbons (GNRs) need to be controlled with atomic precision in order to produce predictable transport properties.[4,5] These stringent requirements pose a major challenge for top-down structuring of GNRs as well as for unzipping carbon nanotubes due to limits in resolution and missing control over the edge passivation.[6,7]

In earlier work, we demonstrated that sub-nm wide GNRs with atomic width control can be achieved via a bottom-up approach consisting of the surface-assisted colligation and subsequent cyclodehydrogenation of suitable precursor monomers that fully determine the GNRs' structure.[8] Scheme 1 describes the synthesis for a specific class of armchair GNRs with a width of $N = 7$ carbon dimer lines (7-AGNRs), which has lately received particular attention. The electronic structure of 7-AGNRs has been determined experimentally, confirming the substantial band gap of 2.3 eV (on the metal substrate) as well as the graphene-derived valence band structure predicted by theory.[9] Very recently, single 7-AGNRs have been picked up at one terminus with the tip of a scanning tunneling microscope (STM), enabling the measurement of the tunneling decay length as a function of bias voltage in a precisely controlled electronic transport experiment.[10]

Scheme 1. On-Surface Synthesis of 7-AGNRs with Plausible Terminations I–IV

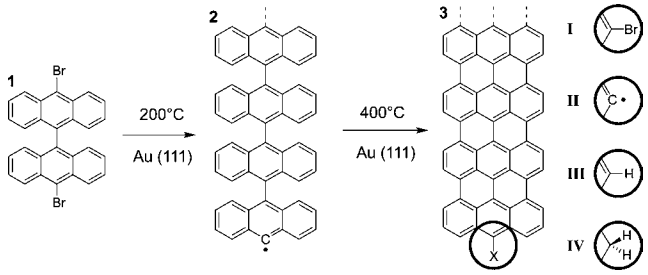

One major challenge remaining in this bottom-up approach is to grow GNRs with lengths significantly exceeding the reported values of around 30 nm.[8] To date, the limiting factor has not been identified. Since growth proceeds by radical addition at the termini of the polymer chain **2**, understanding the chemical structure of the termini is of fundamental importance.[11] In this communication, we focus on the case of the 7-AGNR **3**, whose terminus constitutes a short zigzag edge. We employ density functional theory (DFT) to calculate the electronic structure of finite 7-AGNRs adsorbed on a metal substrate, considering four different termini that are conceivable as products of the on-surface synthesis. STM simulations performed on top of these calculations are then compared with experimental STM images. The results can be generalized to other GNRs fabricated via this approach and indicate that the carbon atoms at the ribbons' termini are passivated by hydrogen (H). We conclude by discussing implications for the polymerization process and giving an outlook on future experiments.

The 7-AGNRs analyzed in this communication were grown on Au(111) (Figure 1) and Ag(111) (Figure S2) following the usual protocol.[11] For imaging of the GNR termini, deposition time was adjusted to yield a GNR coverage below 0.1 monolayers. All images were taken under ultrahigh-vacuum (UHV) conditions with a commercial low-temperature STM from Omicron Nanotechnology at sample temperatures around

Received: November 12, 2012
Published: January 27, 2013

dx.doi.org/10.1021/ja311099k | J. Am. Chem. Soc. 2013, 135, 2060–2063

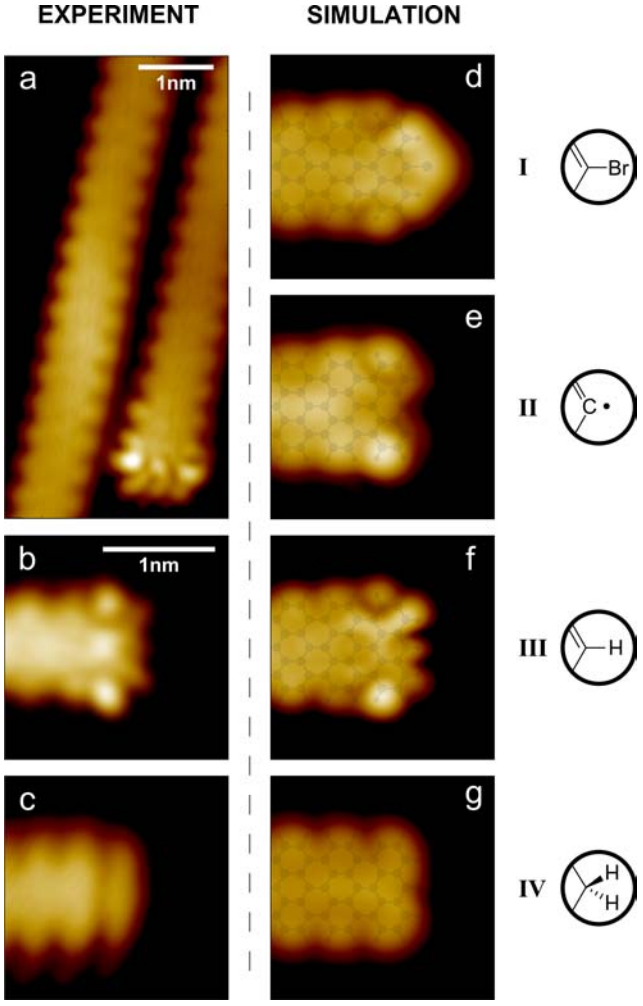

Figure 1. STM images of 7-AGNR termini on Au(111). (a) Characteristic appearance of the terminus (−0.11 V, 210 pA). (b) Close-up (−0.14 V, 50 pA). (c) Featureless terminus (0.10 V, 10 pA). (d–g) STM simulations for the four termini under consideration (−0.3 V, $|\Psi|^2 = 10^{-7}$ Å^{-3}).

5 K. STM images were obtained in constant-current mode (see Figure S3 for constant-height measurements).

Electronic structure calculations were performed within the framework of DFT. We used the CP2K[12] code, which expands the electronic wave functions on an atom-centered Gaussian-type basis set. The substrate was modeled by four Au(111) layers in the repeated slab geometry, and a surface cell of 2 × 4 nm^2 hosted one adsorbed 7-AGNR consisting of three fused precursor monomers **1**. Similar parameters were used for Ag, and all geometries were fully relaxed. STM simulations were performed in the Tersoff–Hamann approximation[13] in constant-current mode (computational details on p S2).

The starting point for our investigation is the characteristic appearance of the 7-AGNRs' termini in STM experiments on Au(111) at low bias (Figure 1a, 1b) that has already been reported before.[10,14] The apparent width increases toward the terminus, which might be described as having two 'eyes' (at the long armchair edge) and three 'antennae' (at the short zigzag edge). Scheme 1 and Figure 1 depict four different chemical terminations of the 7-AGNR that are plausible candidates considering the steps of the 7-AGNR synthesis (Figures 1d–g and S5). In case I, the Br atom has failed to detach from the precursor molecule at the terminus of the ribbon, or has reattached after dissociation. In case II, debromination has occurred as intended, leaving a radical behind that is stabilized by the metal surface. Cases III and IV consider the H passivation of the radical and the addition of a second H atom at the same site. In the following, these candidates are discussed one by one and compared with experiment.

The STM simulation corresponding to case I shows significant electron density on the Br (Figure 1d). This is clearly incompatible with our experimental STM images (Figure 1a, 1b) and rules out this candidate. For the radical (II), the DFT calculation predicts that the carbon atom with the unpaired electron moves down by about 1 Å toward the metal, leading to a buckling of the ribbon (Figure S1). Since the corresponding STM simulation (Figure 1e) does not agree well with experiment either, the question arises whether the radicals have somehow been passivated. This would be compatible with the 7-AGNRs' high mobility, as judged from the impossibility of stably imaging individual ribbons at temperatures above 77 K. Since the samples do not leave UHV conditions, Br and H are the only plausible candidates for the passivating chemical species. Atomic H is generated on the surface during the cyclodehydrogenation step, when eight H are lost per precursor monomer **1** in total.[15] While recombinative desorption of H from Au and Ag surfaces occurs already below room temperature,[16,17] diffusing atomic H may as well passivate the radical termini. We have calculated the total energy difference between a radical ribbon terminus (II) with atomic H on the surface and a H-passivated ribbon terminus (III). We find that H passivation lowers the energy by $|\Delta E| = 1.6–2.1$ eV, where the variation arises from different chemisorption geometries of the radical on the surface. Moreover, the corresponding reaction path is expected to be almost barrierless.

The terminus resulting from such a scenario constitutes a monohydrogenated zigzag edge (III). For infinite monohydrogenated zigzag edges, the well-known single-orbital nearest-neighbor tight-binding model predicts the presence of electronic midgap states that are localized near the edge.[5] The terminus of the 7-AGNR has three zigzag cusps, and here the model predicts the existence of exactly one localized 'edge state'[5] ('Tamm state'[10]), whose corresponding DFT counterpart is shown in Figure 2a. The STM simulation of case III (Figure 1f) fits the experiment very well, reproducing the enlargement of the apparent width toward the terminus as well as the two 'eyes' and the three 'antennae'. In particular, we notice that both simulation (Figure 1f, 2a) and experiment (Figure 1a, 1b) reveal an accumulation of electron density on one of the two carbon sublattices.

Finally, case IV considers the addition of a second H at the same site, resulting in a H_2 termination of the central carbon atom. According to our DFT simulations, this further lowers the total energy by $|\Delta E| = 0.8$ eV, which can be rationalized in an intuitive way by employing Clar's theory:[18] For infinite monohydrogenated zigzag ribbons the aromaticity of Clar formulas is maximized by introducing one unpaired electron every three zigzag cusps.[19] In Figure 2 we apply this reasoning to the monohydrogenated 7-AGNR (III). Considering only the Clar formulas with the maximum and next-highest number of Clar sextets, we identify five carbon sites where the unpaired electron may be introduced. The comparison with the DFT calculation of the finite 7-AGNR in vacuum reveals that these are exactly the carbon sites with the highest weight of the Tamm state. Adding the second H (IV) pairs the electron and

dx.doi.org/10.1021/ja311099k | J. Am. Chem. Soc. 2013, 135, 2060–2063

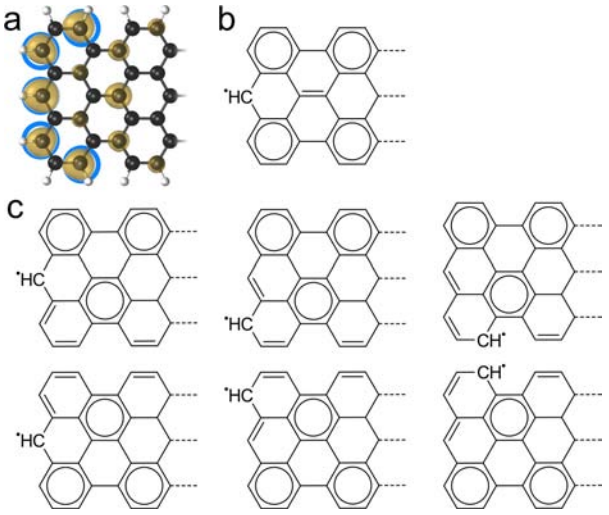

Figure 2. Tamm state at GNR terminus III and corresponding Clar formulas. (a) Constant-density isosurface based on a DFT calculation of the 7-AGNR in vacuum. The five carbon atoms with the highest weight of the Tamm state are highlighted in blue. (b–c) Clar formulas with maximum (b) and next-highest (c) number of Clar sextets.

lowers its energy, thereby removing it from the energetic window studied here via STM (Figure 1c, g).

This is clearly not the case in the typical experimental STM images featuring the Tamm state (Figure 1a, 1b). However, about 15% of the GNR termini in our experiments appear featureless (Figure 1c, Figure S3) as does the STM simulation of case IV (Figure 1g). Featureless termini have also been reported in ref 10, where they are explained by carbon defects that would remove the Tamm state as well. If the featureless termini would indeed correspond to case IV, the energy barrier for removal of the second H should be just 1 eV (see p S2). It should thus be possible to induce dehydrogenation with an STM tip. We have positioned the STM tip on top of a number of featureless ribbon termini and ramped the sample bias at constant height (Figure S4). After this procedure, we consistently find that the termini now display the characteristic features of the Tamm state (Figure S4). This observation cannot be rationalized by the assumption of a carbon defect at the terminus. Instead, it strongly suggests that we were able to transform case IV into case III by removing one H atom.

The identification of H passivation of the ribbon termini has important implications for the understanding of the polymerization process, respectively its interruption. STM images taken after the polymerization step at 200 °C sporadically show bianthryl monomers **1** that already have undergone cyclodehydrogenation, as evidenced by their low apparent height of ∼1.7 Å (Figure S5). This premature cyclodehydrogenation produces atomic H on the surface, which can directly compete with the polymerization reaction by forming a C–H bond at the radical termini of the growing polymer chain **2**, thus inhibiting further radical addition. Our results suggest that for achieving longer GNRs the choice of the monomer and substrate should be optimized in order to suppress dehydrogenation during polymer growth. One possible route involves lowering the polymerization temperature by using appropriate leaving groups as well as solid surfaces that guarantee the required high mobility of the radical species.

In conclusion, we were able to clarify the chemical structure of the termini of bottom-up fabricated[8] GNRs by combining STM simulations and experiments for finite armchair graphene nanoribbons of width $N = 7$ supported on Au(111) and Ag(111) substrates. We demonstrate that the ribbons' termini are passivated by H, which is provided by spontaneous cyclodehydrogenation of monomers or polymer chains. Since the event of H passivation of the radical termini inevitably stops polymer growth, minimizing H loss during the polymerization step may be a way to grow longer GNRs.

■ ASSOCIATED CONTENT

Supporting Information

Method details, STM experiments and simulations on Ag(111), details on tip-induced dehydrogenation, and further supplementary STM images are provided as Supporting Information. This material is available free of charge via the Internet at http://pubs.acs.org.

■ AUTHOR INFORMATION

Corresponding Author

leopold.talirz@empa.ch; carlo.pignedoli@empa.ch

Notes

The authors declare no competing financial interest.

■ ACKNOWLEDGMENTS

This work is supported by the European Science Foundation (ESF) under the EUROCORES Programme EuroGRAPHENE (GOSPEL), by the Swiss National Science Foundation (SNF), and by the Swiss National Supercomputing Centre (CSCS). We thank Ari Seitsonen for fruitful discussions and advice concerning Clar's theory.

■ REFERENCES

(1) Schwierz, F. *Nat. Nanotechnol.* **2010**, *5*, 487–96.
(2) Yang, L.; Park, C.-H.; Son, Y.-W.; Cohen, M.; Louie, S. *Phys. Rev. Lett.* **2007**, *99*, 186801.
(3) Barone, V.; Hod, O.; Scuseria, G. E. *Nano Lett.* **2006**, *6*, 2748–2754.
(4) Nakada, K.; Fujita, M.; Dresselhaus, G.; Dresselhaus, M. *Phys. Rev. B* **1996**, *54*, 17954–961.
(5) Basu, D.; Gilbert, M. J.; Register, L. F.; Banerjee, S. K.; MacDonald, A. H. *Appl. Phys. Lett.* **2008**, *92*, 042114.
(6) Ma, L.; Wang, J.; Ding, F. *ChemPhysChem* **2013**, *14*, 47–54.
(7) Chen, L.; Hernandez, Y.; Feng, X.; Müllen, K. *Angew. Chem., Int. Ed.* **2012**, *51*, 7640–54.
(8) Cai, J.; Ruffieux, P.; Jaafar, R.; Bieri, M.; Braun, T.; Blankenburg, S.; Muoth, M.; Seitsonen, A. P.; Saleh, M.; Feng, X.; Müllen, K.; Fasel, R. *Nature* **2010**, *466*, 470–3.
(9) Ruffieux, P.; Cai, J.; Plumb, N.; Patthey, L.; Prezzi, D.; Ferretti, A.; Molinari, E.; Feng, X.; Müllen, K.; Pignedoli, C. A.; Fasel, R. *ACS Nano* **2012**, *6*, 6930–35.
(10) Koch, M.; Ample, F.; Joachim, C.; Grill, L. *Nat. Nanotechnol.* **2012**, *7*, 713–7.
(11) For graphene edges, chemical information on individual atoms has also been obtained through energy-loss near-edge fine structure analysis: Suenaga, K.; Koshino, M. *Nature* **2010**, *468*, 1088–90.
(12) The CP2K developers group. http://www.cp2k.org/ (accessed March 2012).
(13) Tersoff, J.; Hamann, D. *Phys. Rev. B* **1985**, *31*, 805–13.
(14) Linden, S.; Zhong, D.; Timmer, A.; Aghdassi, N.; Franke, J.; Zhang, H.; Feng, X.; Müllen, K.; Fuchs, H.; Chi, L.; Zacharias, H. *Phys. Rev. Lett.* **2012**, *108*, 216801.
(15) Blankenburg, S.; Cai, J.; Ruffieux, P.; Jaafar, R.; Passerone, D.; Feng, X.; Fasel, R.; Pignedoli, C. A. *ACS Nano* **2012**, *6*, 2020–2025.
(16) James, M. N. G.; Williams, G. J. B. *Acta Crystallogr., Sect. B: Struct. Crystallogr. Cryst. Chem.* **1973**, *29*, 1172–74.

(17) Murphy, M.; Hodgson, A. *Surf. Sci.* **1996**, *368*, 55−60.
(18) Clar, E. *The Aromatic Sextet*; Wiley: London, 1972.
(19) Wassmann, T.; Seitsonen, A. *J. Am. Chem. Soc.* **2010**, *132*, 3440−51.